Solid State Ionics xxx (2016) xxx–xxx

Contents lists available at ScienceDirect

Solid State Ionics

journal homepage: www.elsevier.com/locate/ssi

Analysis and Application of Distribution of Relaxation Times in Solid State Ionics

Bernard A. Boukamp [a,*], Aurélie Rolle [b,c]

[a] University of Twente Fac. of Science and Technology & MESA+ Institute for Nanotechnology, P.O. Box 217, 7500 AE, Enschede, The Netherlands
[b] Univ. Lille Nord de France, F-59000, Lille, France
[c] CNRS UMR8181, Unité de Catalyse et Chimie du Solide UCCS, ENSCL, Université Lille 1, F-59652, Villeneuve d'Ascq, France

ARTICLE INFO

Article history:
Received 27 July 2016
Received in revised form 4 October 2016
Accepted 17 October 2016
Available online xxxx

Keywords:
Distribution of relaxation times
Electrochemical impedance spectroscopy (EIS)
Havriliak-Negami dispersion
Gerischer dispersion
SOFC cathode

ABSTRACT

Three methods for obtaining a Distribution (Function) of Relaxation Times (DFRT) are compared, Fourier transform (FT), Tikhonov regularization (TR) and a multiple-(RQ) CNLS-fit. The FT method was written in the programming package 'Borland Delphi', for the Tikhonov regularization (TR) a freely available MatLab application (DRTtools) was used. The CNLS-fit was performed with the EqCwin95 software. Where possible the DFRT's were compared with an exact, calculated τ-domain representation of the model impedance. Practical use of the DFRT is demonstrated in the analysis of the impedance of a $Ca_3Co_4O_{9+\delta}$-$Ce_{0.9}Gd_{0.1}O_{0.95}$ composite cathode (CCO-CGO). The comparison shows that the FT and TR methods have problems in presenting the sharp and asymmetric peak of the DFRT of a Gerischer dispersion. In that case the multiple-(RQ) CNLS-fit presents too many peaks. Reconstruction of the impedance from the DFRT and comparing it to the original data set is a useful validation procedure for the DFRT.

1. Introduction

Electrochemical Impedance Spectroscopy (EIS) is a powerful tool in Solid State Electrochemistry [1]. It commonly involves fitting a viable equivalent circuit (EC) to the measurement data set, using a nonlinear least squares (CNLS) procedure [1–5]. The EC can be built with known electrical analogues, such as resistance, capacitance and inductance, but also with more complex functions like semi-infinite and bounded diffusion (Warburg type) elements [1]. Although often good results are obtained with the EC-CNLS analysis, in complicated cases, such as porous and/or composite electrodes, it may be difficult to find an appropriate EC.

An alternative way for EIS data analysis is a transformation into a Distribution (Function) of Relaxation Times (DFRT), also known as a transformation to the τ-domain. This is a model independent representation that emphasises the larger contributions to the frequency dispersion, visible as more or less sharp peaks. The peak positions define the major time constants of the electrochemical cell. Following the trends of peak position and peak height as function of temperature, partial pressure and/or polarization provides information on the electrochemical processes [6]. The distribution of relaxation times concept has already been applied in the past in the study of dielectric properties and ionic conduction in solids, see e.g. Franklin and De Bruin [7]. The DFRT, $G(\tau)$, can be obtained from solving the following expression:

$$Z(\omega_i) = R_\infty + R_p \int_{-\infty}^{\infty} \frac{G(\tau)}{1 + j\omega_i\tau} \, \mathrm{d}\, \ln\tau \qquad (1)$$

with $Z(\omega_i)$ the data set, R_∞ the high frequency cut-off resistance, R_p the polarization resistance or overall resistance of the dispersion. $G(\tau)$ is a normalized function with $\int_{-\infty}^{\infty} G(\tau) \, \mathrm{d}\ln\tau = 1$.

Unfortunately, this procedure is known as an 'ill-posed inverse problem', which means that there are many possible solutions for $G(\tau)$. A major restriction applied here is that $G(\tau)$ must be positive for all τ, which certainly diminishes the number of possible functions. Furthermore, one should try to find the most simple expression or 'the best optimized' curve. Several routes to the τ-domain have been presented recently: Fourier Transform (FT) [6,8], Maximum Entropy [9,10] and Tikhonov Regularization (TR) [11–13]. All these methods have in common that a special parameter must be adjusted to obtain an agreeable DFRT representation. The focus is then on minimizing unwanted oscillations and obtaining a (mostly) positive distribution of $G(\tau)$ values. A critical review of the FT-method, applied to Solid State Electrochemistry examples, has recently been presented by the first author [8].

The Fourier transform method presented by Schichlein et al. [6] uses only the imaginary part of the impedance data. Data validation with a

* Corresponding author at: University of Twente, Science & Technology, P.O. Box 217, Bldg Carré 3.251, 7500, AE, Enschede, Netherlands.
E-mail address: b.a.boukamp@utwente.nl (B.A. Boukamp).

http://dx.doi.org/10.1016/j.ssi.2016.10.009
0167-2738/

Kramers-Kronig test [14] is then an important requirement. The expression to be solved becomes then:

$$Z_{im}(\omega) = -R_p \int_0^{\infty} \frac{\omega\tau}{1+\omega^2\tau^2}\gamma(\tau)\ \mathrm{d}\ \tau \tag{2}$$

A change of variables with $x = \ln\omega/\omega_0$; $y = \ln\omega\tau$; $g(y-x) = \tau\cdot\gamma(\tau) = G(\tau)$, results in a convolution integral [6]:

$$Z_{im}(\omega) = -\frac{R_p}{2}\int_{-\infty}^{\infty} \mathrm{sech}(y)\cdot g(y-x)\ \mathrm{d}y \tag{3}$$

ω_0 is the centre frequency of the data set. The deconvolution is performed with a Fourier transform which yields the Fourier transform of the DFRT. Schichlein et al. [6] used discrete fast Fourier transforms (FFT) to obtain the DFRT, limiting the FFT to the actual frequency range:

$$\overline{Z_{im}(s)} = -NT\frac{R_p}{2}\ \overline{\mathrm{sech}(s)}\cdot\overline{G(s)} \tag{4}$$

Where N is the number of data and T is the sampling interval: $T = (N\text{-}1)^{-1}\ln(\omega_{max}/\omega_{min})$. In an effort to optimize this FT-procedure, the first author has applied an extension method to the low and high frequency part of the imaginary data set. This allowed an integration from -∞ to +∞ as will be briefly explained in the next section, see also ref. [8]. The FT-integrations were performed through quadratic interpolations.

In this contribution three methods for obtaining a DFRT will be presented and compared: *i*, the FT-method as presented in ref. [8]; *ii*, the Tikhonov regularization as described by Wan et al. [13]; *iii*, the multiple-(RQ) CNLS-fit which has been presented also in ref. [8]. The user friendly MatLab application 'DRTtools', developed by Wan [15], was used for the TR-transform. The CNLS-fit of the multiple-(RQ) model was performed with the software package 'EqCwin95' [16]. The comparisons will be carried out on three simple examples for which an exact DFRT is available: a simple R(RQ)(RQ) circuit [2,17], a Havriliak-Negami dispersion (H-N) [18–20] and a Gerischer response [21]. A more practical comparison is presented with an actual EIS measurement on a $Ca_3Co_4O_{9+\delta}$-$Ce_{0.9}Gd_{0.1}O_{0.95}$ (CCO-CGO) SOFC cathode. A detailed impedance study on a range of compositions of the CCO-CGO cathode by Rolle et al. has recently been published [22].

2. Simple R(RQ)(RQ) model

The R(RQ)(RQ) follows the 'circuit description code' (CDC) developed by Boukamp [2,17]. *R* presents a resistance, the (RQ) a parallel combination of a resistance and a constant phase element (CPE). The dispersion relation for the CPE, presented by the 'Q', is given in admittance representation by:

$$Y_{CPE}(\omega) = Y_0(j\omega)^{\varphi} \tag{5}$$

For $\varphi = 1$ it represents a capacitance with $C = Y_0$; for $\varphi = 0$, a resistance with $R = Y_0^{-1}$; for $\varphi = -1$, an inductance with $L = Y_0^{-1}$; and for $\varphi = ½$ a Warburg or semi-infinite diffusion. The parallel combination (RQ), also known as 'Zarc', has an exact representation in τ–space [23]:

$$R\cdot G(\tau) = \frac{R}{2\pi}\frac{\sin([(1-\varphi)\pi]}{\cosh[\varphi\ln(\tau/\tau_0)] - \cos[(1-\varphi)\pi]} \tag{6}$$

The time constant of the (RQ) is given by: $\tau_0 = \sqrt[\varphi]{R\cdot Y_0}$. The area under the curve of Eq. (6) versus lnτ is equal to *R*. Fig. 1A shows the impedance of the simulation, Fig. 1B presents the exact DFRT for this R(RQ)(RQ) circuit.

The DFRT obtained with the Tikhonov regularization program [15], using the default settings, is also shown in Fig. 1B. Increasing the regularization parameter (RP) from 10^{-3} (default) to 10^{-2} or higher, removes the small oscillations at ~10 μs and 1 ms, but it also lowers the peak heights and slightly increases the peak width.

The frequency extrapolation procedure for the Fourier transformation [8] is schematically presented in Fig. 2A. A limited number of data points in both end regions are fitted with simple R(RQ) circuits, which then provide extrapolations to lower (or higher) frequencies. For a low enough value of ω_{low} the extrapolation can be simplified to an analytical FT (from -∞ to $\ln\omega_{low}$), with $x = \ln\omega$:

$$Q_{ll}\int_{-\infty}^{x_{ll}} e^{\varphi x}\cdot e^{-jsx}\,\mathrm{d}x = Q_{ll}\cdot e^{\varphi x_{ll}}\left[\frac{\varphi\cos sx_{ll} + s\sin sx_{ll}}{s^2+\varphi^2} + j\frac{s\cos sx_{ll} - \varphi\sin sx_{ll}}{s^2+\varphi^2}\right] \tag{7}$$

Here $Q_{ll} = R^2Y_0\cdot\sin(\varphi\pi/2)$ and $x_{ll} = \ln\omega_{low}$. *R*, Y_0 and φ are defined by the low frequency extension. A similar procedure leads to an analytical FT expression for the high frequency extrapolation, see ref. [8] for full details. The Fourier transform, $\overline{G(\tau)}$, shows strong oscillations in the end regions of *s*. Hence for the reverse transform a window filter is needed to obtain a useable DFRT presentation. A standard filter is the Hann window [24], with s_{max} setting the filter width:

$$W_H(s) = \frac{1}{2}\left(1+\cos\left(\frac{\pi\ s}{s_{max}}\right)\right),\quad |s|\le s_{max} \qquad W_H(s) = 0,\quad |s| > s_{max} \tag{8}$$

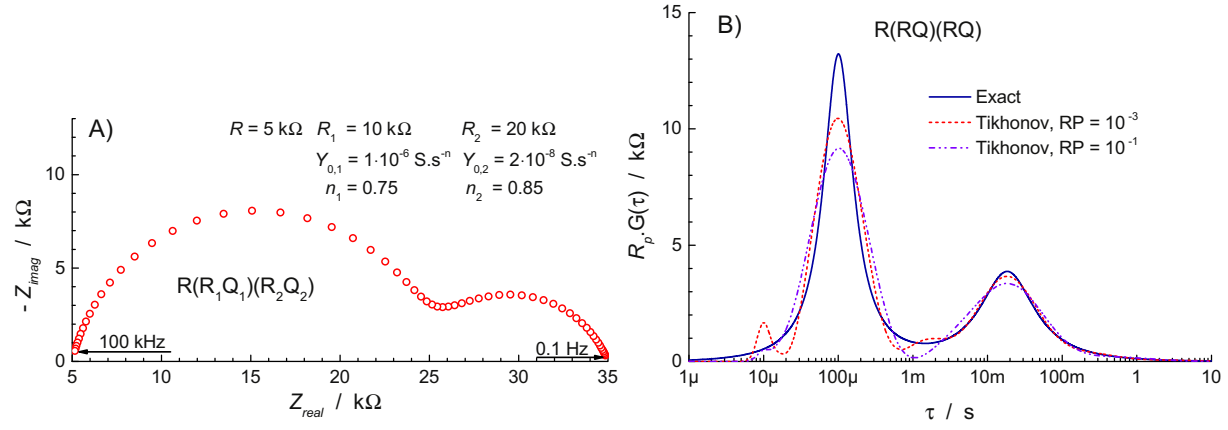

Fig. 1. A) Impedance simulation of the R(RQ)(RQ) model. B) Exact DFRT with two TR simulations. RP = regularization parameter.

Please cite this article as: B.A. Boukamp, A. Rolle, Analysis and Application of Distribution of Relaxation Times in Solid State Ionics, Solid State Ionics (2016), http://dx.doi.org/10.1016/j.ssi.2016.10.009

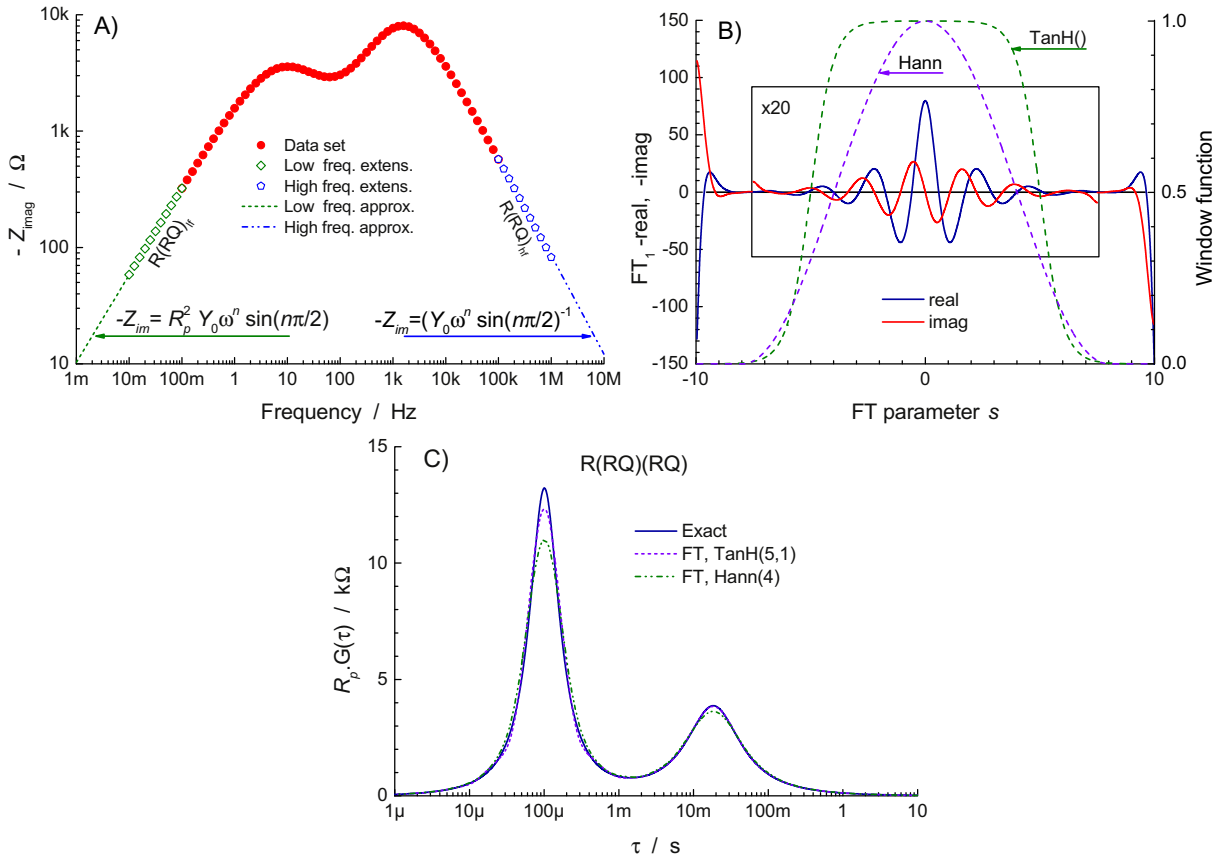

Fig. 2. A) Frequency extension model for the FT transform. B) first FT with Window functions. The central part has been magnified 20 times for clarity. C) Inverse FT for $R_p \cdot G(\tau)$ for two Window functions. Exact DFRT is presented by the continuous line.

In ref. [8] a different filter was suggested, which is based on a tangent hyperbolic function, providing a more flat filter value of almost 1 in the central part:

$$W_T(s) = \frac{(\tanh[\beta(\alpha+s)]+1)(\tanh[\beta(\alpha-s)]+1)}{4} \quad (9)$$

This window function, $W_T(s)$, is represented further by 'TanH(α,β)', where α is the width (at half height) and β represents the steepness of the sides of the window.

The first Fourier transform to $\overline{G(s)}$, FT_1, is presented in Fig. 2B, together with the used filter windows, Eqs. (8)–(9). The strong deviations in the end regions clearly show the need to apply a window function in the revers transform. The derived DFRT's are presented in Fig. 2C, showing a very good similarity to the exact DFRT, although the peak heights are somewhat lowered. It is obvious that the multiple-(RQ) CNLS method does not apply to this example.

3. Havriliak-Negami dispersion

The Havriliak-Negami dispersion is an empirical function derived to describe the dielectric properties of polymers [18–20], but it is also used in the impedance representation:

$$Z(\omega) = Z_\infty + \frac{R_0}{\left[1+(j\omega\tau_0)^\beta\right]^\gamma} \quad (10)$$

Eq. (10) is a general expression (similar to the CPE). With $\gamma = 1$ it represents a (RQ) or 'Zarc' dispersion, also known as the Cole-Cole dispersion [25]. With $\beta = 1$ it represents the Cole-Davidson dispersion expression [26]. But for $\gamma = 0.5$ and $\beta = 1$ it represents the well-known Gerischer dispersion [1,21] or chemical impedance [27]. Eq. (10) can be separated in a real and imaginary part through:

$$Z(\omega) = \frac{R_0}{\left[1+(j\omega\tau_0)^\beta\right]^\gamma} = \frac{R_0}{(a+jb)^\gamma} \quad (11)$$

With:

$$a = 1 + \cos\left(\frac{\beta\pi}{2}\right)(\omega\tau_0)^\beta;\ b = \sin\left(\frac{\beta\pi}{2}\right)(\omega\tau_0)^\beta \quad (12)$$

$(a+jb)^\gamma$ can be expanded to:

$$(a+jb)^\gamma = \left\{\cos\left[\gamma\cdot\operatorname{atan}\left(\frac{b}{a}\right)\right] + j\sin\left[\gamma\cdot\operatorname{atan}\left(\frac{b}{a}\right)\right]\right\}\left(a^2+b^2\right)^{\gamma/2} \quad (13)$$

This allows easy simulation of the H-N type dispersion. Fig. 3A presents a H-N model with $\beta = 0.7$ and $\gamma = 0.8$ over the frequency range 0.1 mHz – 10 kHz. For the multiple-(RQ) CNLS-fit four (RQ)'s in series were used to fit the H-N model. The residual fit errors of <0.1% are well below the average measurement noise, see insert in Fig. 3A.

An exact formula for the τ-domain representation of the H-N dispersion has also been presented by several authors [13,18–20] as:

$$G(\tau) = \frac{1}{\pi}\left(\frac{\tau}{\tau_0}\right)^{\beta\gamma} \frac{\sin(\gamma\theta)}{\left[1+2\cos(\pi\beta)\left(\frac{\tau}{\tau_0}\right)^\beta + \left(\frac{\tau}{\tau_0}\right)^{2\beta}\right]^{\gamma/2}} \quad (14a)$$

Please cite this article as: B.A. Boukamp, A. Rolle, Analysis and Application of Distribution of Relaxation Times in Solid State Ionics, Solid State Ionics (2016), http://dx.doi.org/10.1016/j.ssi.2016.10.009

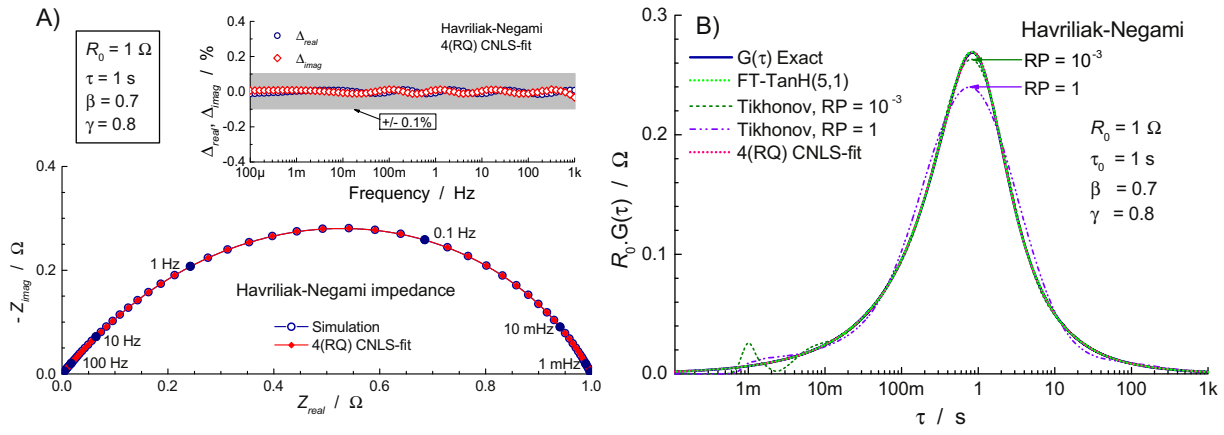

Fig. 3. A) Havriliak-Negami impedance simulation. The 4-(RQ) CNLS-fit is also displayed. Insert presents the relative errors. B) Exact H-N DFRT (Eqs. (14a)-(14b)) together with the FT-TanH, TR and 4-(RQ) DFRT's. RP = regularization parameter for the TR transform.

$$\text{with: } \theta = \operatorname{atan}\left(\frac{\sin(\pi\beta)}{\left(\frac{\tau}{\tau_0}\right)^{\beta} + \cos(\pi\beta)}\right) \tag{14b}$$

Fig. 3B shows the exact DFRT of the H-N model of Fig. 3A. Both the 4(RQ) CNLS-fit transform and the FT-transform fall virtually on top of the exact curve. The Tikhonov transform is presented with RP = 10^{-3}, which shows the basic curve with a somewhat lower peak height and an oscillation for τ = 1–2 ms. Increasing the RP to 1 lowers the peak height and diminishes the oscillations (also shown).

4. DFRT of a parallel R-C

A (RC) circuit has just a single time constant with $\tau_{(RC)} = R \cdot C$. The first Fourier transform, $FT_1 = \overline{G(s)}$, results in a horizontal straight line. The back transform is a δ-function at $\tau = \tau_{(RC)}$, which should also follow from Eq. (6) for $\varphi \to 1$. This implies that information on R ,i.e. area under

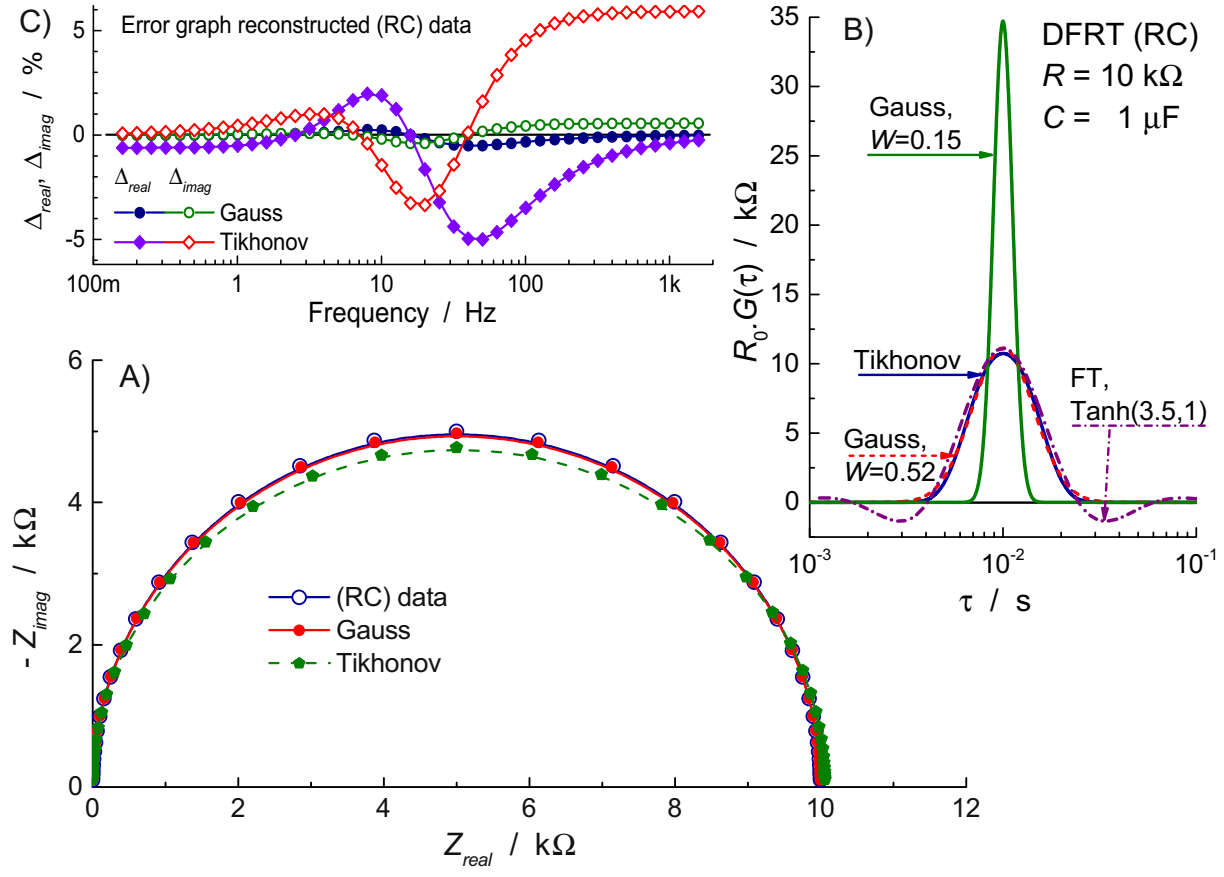

Fig. 4. A) Impedance of a (RC) circuit. B) FT-, TR-DFRT and Gaussian representations. C) Relative error plot for the TR and Gaussian (W = 0.15) reconstructions.

Please cite this article as: B.A. Boukamp, A. Rolle, Analysis and Application of Distribution of Relaxation Times in Solid State Ionics, Solid State Ionics (2016), http://dx.doi.org/10.1016/j.ssi.2016.10.009

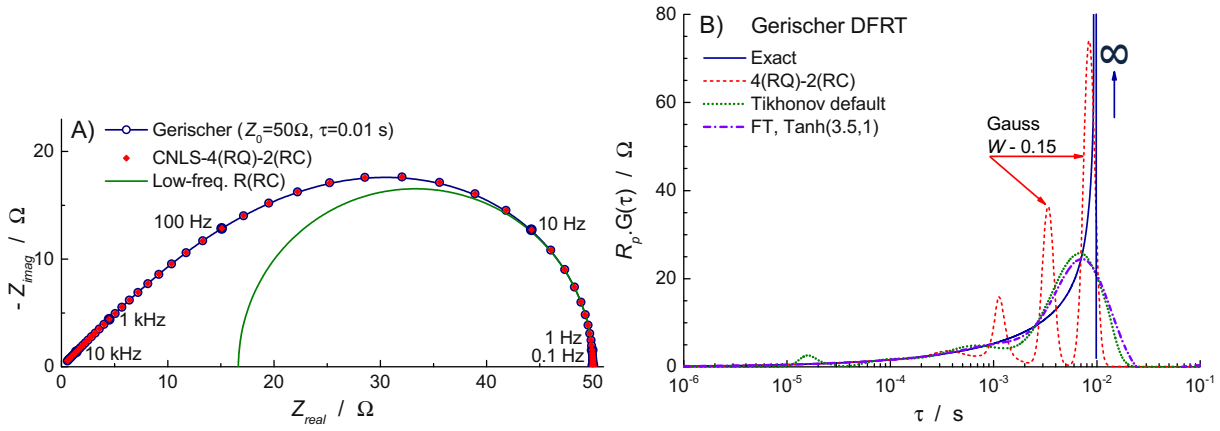

Fig. 5. A) Gerischer impedance with low frequency R(RC) approximation and 4-(RQ)-2-(RC) CNLS-fit. B) Exact Gerischer DFRT (continuous line) and the FT- and TR-transforms. The multi-(RQ) shows three distinct peaks.

the curve, is lost. Due to the limited range of s in the reverse transform, the integration is truncated, or limited through application of a filter window (see Section 2). The filter 'softens' the delta function into a more Gaussian type shape. Fig. 4A shows the impedance of a (RC), the Tikhonov DFRT (default settings) is shown in Fig. 4B. It closely matches a Gaussian function:

$$R \cdot G(\tau) = \frac{R}{W\sqrt{\pi}} \cdot e^{-\left(\frac{\ln(\tau/\tau_0)}{W}\right)^2} \tag{15}$$

W defines the width of the Gaussian. For the TR-DFRT $W = 0.52$, which amounts to a FWHM of 0.38 decade in τ. The FT-DFRT with a window setting of TanH(3.5,1) follows the TR-DFRT for the main part, but shows negative excursions on both sides of the peak.

In the multiple-(RQ) CNLS-fit method a (RC) component cannot be automatically presented in a $R{\cdot}G(\tau)$ representation. As suggested in ref. [8], a Gaussian function can be used to replace the δ-function. The width parameter has (rather arbitrarily) been set at $W = 0.15$, which gives a sharp peak with a FWHM of 0.11 decade in τ. For both the TR-DFRT and the Gaussian function with $W = 0.15$, the impedances have been reconstructed using Eq. (1). These are also displayed in Fig. 4A. The Gaussian reconstruction shows a small relative error of <1%, while the Tikhonov reconstruction shows a significant error of up to 6% at higher frequencies, see Fig. 4C. This shows that in the multiple-(RQ) transform the replacement of a (RC) with a sharp Gaussian function in the DFRT leads to quite acceptable results.

5. Gerischer dispersion

As indicated above, the Gerischer dispersion is a special case of the Havriliak-Negami relation, with $\gamma = ½$ and $\beta = 1$:

$$Z_G(\omega) = \frac{Z_0}{\sqrt{1 + j\omega\tau_0}} = \frac{Z_0'}{\sqrt{K_a + j\omega}} \tag{16}$$

K_a represents in the right hand part a reaction rate ($K_a = \tau_0^{-1}$) [21]. Using the H-N Eqs. (14a–b) the DFRT for the Gerischer can be derived for $\gamma = ½$ and $\beta = 1$. The derivation is nontrivial, it requires taking the limit of Eqs. (14a)–(14b) for $\beta \rightarrow 1$. This results in the following simple and ***exact*** expression for the DFRT:

$$G(\tau) = \frac{1}{\pi}\sqrt{\frac{\tau}{\tau_0 - \tau}}, \quad \tau \le \tau_0 \quad \wedge \quad G(\tau) = 0, \tau > \tau_0 \tag{17}$$

Fig. 5A shows the impedance representation of a Gerischer dispersion. For $\omega < 0.1 \cdot \tau_0^{-1}$ the low frequency end can be modelled with a $R_1(R_2C)$ circuit with $R_1 = ⅓\, Z_0$, $R_2 = ⅔\, Z_0$ and $C = (9/8)\, \tau_0 \cdot Z_0^{-1}$, see Fig. 5A.[1] In τ-space this R(RC) circuit will yield a δ-function at τ_0. Hence it is no surprise that the G(τ) function shows a singularity for $\tau = \tau_0$.

Both the FT and TR transforms produce a broad asymmetric curve, unlike the asymptotic shape of the exact G(τ), see Fig. 5B. The Gerischer impedance can be very well fitted with a 4(RQ)-2(RC) circuit with relative errors <0.1%, well below the average noise level. But the DFRT calculated with the CNLS-parameters shows three sharp peaks instead of one at the τ_0 position.

In fact, taking $\gamma = ½$ and letting β go from 0.7 to 1 shows that the TR transformation leads to one broad peak with a diminishing relative peak height. Up to $\beta = 0.95$, the FT follows the exact DFRT quite closely (results not shown). For $\beta = 1$ (Gerischer) also the FT-method is not able to reproduce the exact DFRT, see Fig. 5B. The 5(RQ) CNLS transform shows with increasing β up to 0.95 an increasingly sharper peak, very near the exact position of τ_0, while developing a second, smaller peak at a 2–2.5 times smaller position of τ_0. For $\beta = 1$, six (RQ) elements are needed (see above). Hence, none of the three methods reproduces the exact Gerischer DFRT properly, the FT and TR methods result in broad shapes, the Multiple-(RQ) in multiple sharp peaks instead of one peak. The reconstructed impedance for the TR (with RP = 10^{-3}) is quite close to the original Gerischer dispersion up to 10 kHz (relative errors <2.5%). The FT-reconstruction is worse, above 100 Hz (~τ_0^{-1}) the relative errors deviate strongly outside the 2.5% limit.

6. CCO-CGO SOFC Cathode

In a recent study by Rolle et al. [22] the electrode polarization of a series of CCO-CGO composite cathodes was studied. The frequency dispersions of the symmetric cells were rather featureless. Fig. 6A shows a typical example of the 70 wt% CCO - 30 wt% CGO composition at 700 °C as raw data and with the instrumental inductance subtracted. The FT- and TR-DFRT's of this dispersion were almost identical, except for small oscillations in the end regions, see Fig. 6C. Both DFRT's also showed no clear peaks. In contrast, the multiple-(RQ) fit, with relative errors <0.2%, resulted in two clear and sharp peaks, while the tail for $\tau < 10^{-3}$ s followed the FT- and TR-curves, see Fig. 6C. The impedance reconstructed from the TR-DFRT, however, also matched the data quite closely up to ~10 kHz, see insert in Fig. 6A.

As CCO is a mixed conductor, the presence of a Gerischer element could be expected. The peak at ~0.1 s was assigned to a bulk redox process (C_{redox} ~ 80–100 F·cm^{-3}, [22]). Further analysis, based on the 5(RQ)-DFRT, resulted in a Gerischer containing EC, as presented in Fig. 6B. The high frequency $(RQ)_1$ and $(RQ)_2$ in Fig. 6B are diffusion related

[1] Note: this is a phenomenological relation observed for $\omega\tau_0$ smaller than ~$2{\cdot}10^{-2}$.

Please cite this article as: B.A. Boukamp, A. Rolle, Analysis and Application of Distribution of Relaxation Times in Solid State Ionics, Solid State Ionics (2016), http://dx.doi.org/10.1016/j.ssi.2016.10.009

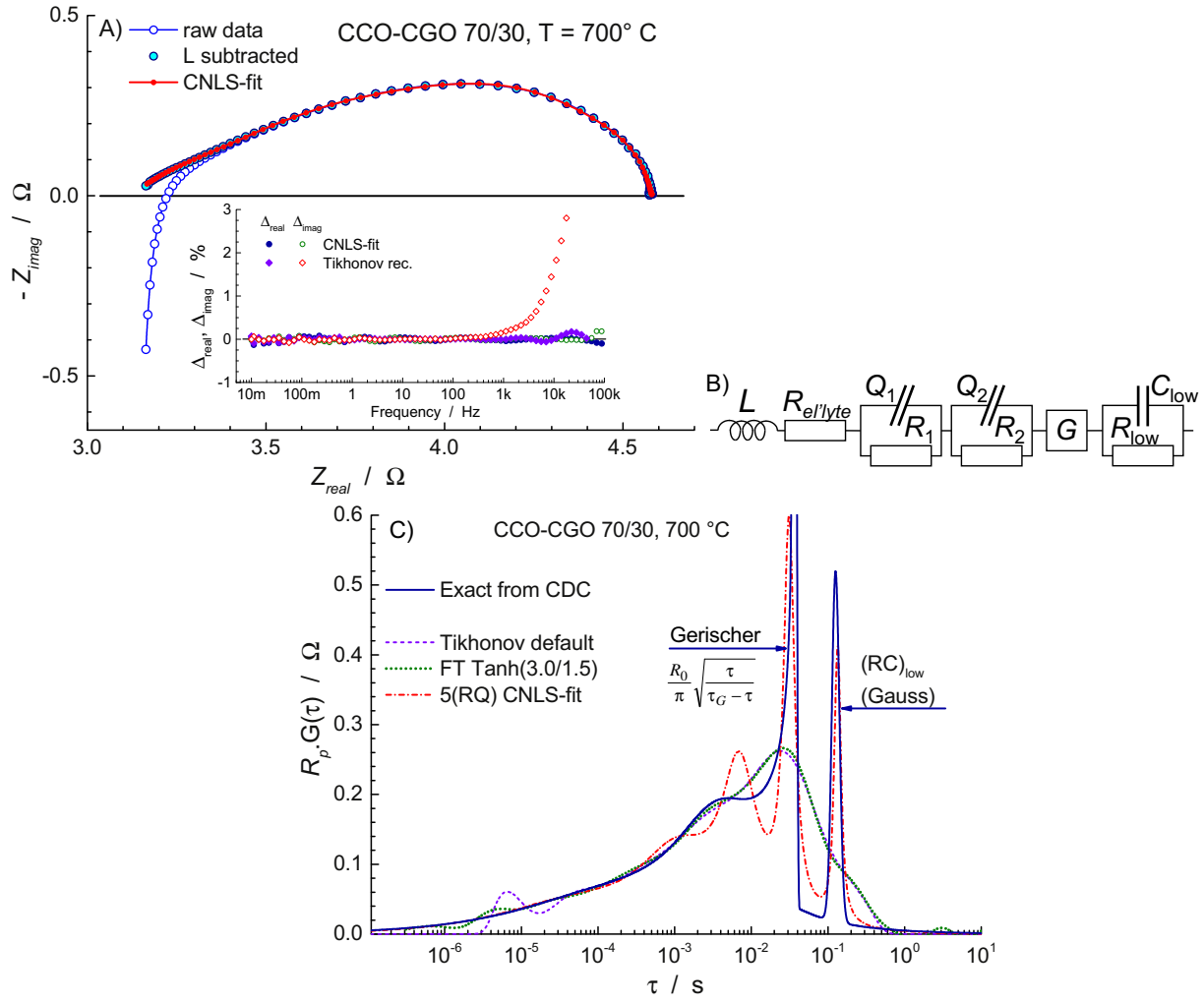

Fig. 6. A) Typical impedance and CNLS-fit of a 70–30 CCO-CGO composite cathode. The insert shows the relative errors of the CNLS-fit and the TR-reconstruction. B) General EC for the CNLS-fit, 'G' denotes the Gerischer. C) Exact DFRT obtained from CNLS-fit with this EC. Also shown the FT-, TR- and the 5(RQ)-DFRT's.

(φ_1 and φ_2 ~ 0.5). The exact DFRT, based on the CNLS-fit with the EC of Fig. 6B, is also presented in Fig. 6C. The multiple-(RQ) transform, i.e. the 5(RQ) CNLS-fit, shows a quite reasonable match with the exact DFRT, reproducing the two major peaks quite well.

The equivalent circuit of Fig. 6B could be used in the CNLS-fits for all compositions at all temperatures. This is well demonstrated in the Arrhenius graph of the time constants for the low frequency (RC), $\tau_{(RC)}$, and the Gerischer, τ_0, as presented in Fig. 7. They fall in two narrow bands for all compositions. This indicates that both time constants represent materials properties, virtually independent of composition [22].

7. Discussion

It is remarkable that the Fourier transform (FT) and the Tikhonov regularization (TR) show quite identical results, except for the low-τ end-region where oscillations might occur. But both are not capable of correctly reproducing sharp peaks that are closely spaced, as is shown in the CCO-CGO cathode example. This is in contrast with the DFRT obtained for a complex model function by Schichlein et al. (see ref. [6], Fig. 4) or Boukamp (ref. [8], Fig. 3) which clearly showed all six time constants in well separated peaks. Decreasing the window width in the FT, or increasing the regularization parameter in the TR has the same effect: removing oscillations, lowering the peak heights and increasing the peak width. The Tikhonov DRTtools MatLab application has many parameter options, which have not yet been explored fully in this investigation. In general it was found that the 'default setting' provided good results, but sometimes one needs to increase the regularization parameter to remove oscillations. The FT-method, as presented in ref.

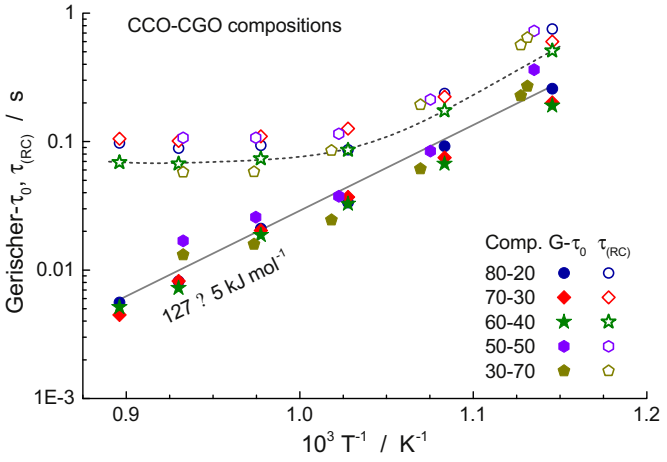

Fig. 7. Arrhenius graph of the two major time constants of the CCO-CGO compositions. The grey line represents a fit to all τ_0 data. The dashed line serves as a guide to the eye. (Results adapted from Rolle et al. [22]).

Please cite this article as: B.A. Boukamp, A. Rolle, Analysis and Application of Distribution of Relaxation Times in Solid State Ionics, Solid State Ionics (2016), http://dx.doi.org/10.1016/j.ssi.2016.10.009

[8], requires extra fitting procedures for the extension of the frequency range, which makes it less efficient to use.

In contrast, the multiple-(RQ) transform method is capable of presenting sharp peaks. The necessary replacement of the δ-function for a (RC) contribution by a Gaussian function, Eq. (15), has only a small effect on the reconstruction of the impedance (see Fig.4). However, this method also has its limitations, as a 'negative (RQ)' might occur in the fit procedure, i.e. both R and Y_0 are negative with a positive τ_0. It is also prone to presenting more peaks than to be expected, see Section 5 and ref. [8].

An alternative method has been presented by Hershkovitz et al. in ref. [28]. In this method a number of functions from a large pool of general expressions is combined to create a DFRT. In the optimization procedure the DFRT is fitted via a reconstruction (Eq. 1) to the impedance data, using an advanced evolutionary programming technique. This method has a large degree of freedom to arrive at the optimum, but the problem is then to assign physical meaning to the fitted functions [28]. It has, however, the advantage of using realistic distribution functions that have no (simple) analytic counterpart in the frequency domain. It is obvious that comparing the impedance reconstruction of the DFRT with the measured data is an important validation procedure for all methods.

8. Conclusions

As stated in the introduction, transforming an impedance into a DFRT is an 'ill-posed inverse problem'. The results presented so far have only emphasized this notion. All of the three methods have their flaws, the FT- and TR-methods seem to suppress sharp peaks, e.g. from a (RC) or Gerischer contribution. The multiple-(RQ) method is able to present these peaks better, but it is also prone to presenting too many peaks. While the DFRT's, obtained with the different methods, can be quite dissimilar, the reconstructed impedances present often a quite reasonable match to the measurements. Hence, it is clear that there is no guaranty that the obtained DFRT is the 'only correct one'. Caution must be exercised with the interpretation of DFRT's.

Acknowledgement

The authors want to express their gratitude to Dr. Wan for sharing on the Internet the user friendly MatLab application 'DRTtools'.

References

[1] B.A. Boukamp, Solid State Ionics 169 (2004) 65–73.
[2] B.A. Boukamp, Solid State Ionics 20 (1986) 31–44.
[3] J.R. Macdonald, L.D. Potter Jr., Solid State Ionics 24 (1987) 61–79.
[4] K.E.D. Wapenaar, J. Schoonman, Solid State Ionics 5 (1981) 637–640.
[5] J.R. Dygas, G. Fafilek, H. Durakpasa, M.W. Breiter, J. Appl. Electrochem. 23 (1993) 553–558.
[6] H. Schichlein, A.C. Müller, M. Voigts, A. Krügel, E. Ivers-Tiffée, J. Appl. Electrochem. 32 (2002) 875–882.
[7] A.D. Franklin, H.J. de Bruin, Phys. Status Solidi A 75 (1983) 647–656.
[8] B.A. Boukamp, Electrochim. Acta 154 (2015) 35–46.
[9] T. Hörlin, Solid State Ionics 67 (1993) 85–96.
[10] T. Hörlin, Solid State Ionics 107 (1998) 241–253.
[11] S. Kazlauskas, A. Kežionis, T. Šalkus, A.F. Orliukas, Solid State Ionics 231 (2013) 37–42.
[12] M. Saccoccio, T.H. Wan, C. Chen, F. Ciucci, Electrochim. Acta 147 (2014) 470–482.
[13] T.H. Wan, M. Saccoccio, C. Chen, F. Ciucci, Electrochim. Acta 184 (2015) 483–499.
[14] B.A. Boukamp, J. Electrochem. Soc. 142 (1995) 1885–1894.
[15] DRTtools and manual, https://sites.google.com/site/drttools/.
[16] A. Wisse, B.A. Boukamp, EqCwin95, http://www.wisseq.nl/portfolio.aspx (in Dutch).
[17] CDC_Explained.pdfavailable from www.utwente.nl/tnw/ims/publication/downloads/.
[18] F. Alvarez, A. Alegra, J. Colmenero, Phys. Rev. B 44 (1991) 7306–7312.
[19] A. Bello, E. Laredo, M. Grimau, Phys. Rev. B 60 (1999) 12764–12774.
[20] A. Bello, E. Laredo, M. Grimau, J. Chem. Phys. 113 (2000) 863–868.
[21] B.A. Boukamp, H.J. Bouwmeester, Solid State Ionics 157 (2003) 29–33.
[22] A. Rolle, H.A.A. Mohamed, D. Huo, E. Capoen, O. Mentré, R.-N. Vannier, S. Daviero-Minaud, B.A. Boukamp, Solid State Ionics 294 (2016) 21–30.
[23] F. Dion, A. Lasia, J. Electroanal. Chem. 475 (1999) 28–37.
[24] S.D. Stearns, Digital signal analysis, Hayden Book Company, New Jersey, 1975 93.
[25] K.S. Cole, R.H. Cole, J. Chem. Phys. 9 (1941) 341–351.
[26] D.W. Davidson, R.H. Cole, J. Chem. Phys. 19 (1951) 1484–1490.
[27] Y. Lu, C. Kreller, S.B. Adler, J. Electrochem. Soc. 156 (2009) B513–B525.
[28] S. Hershkovitz, S. Baltianski, Y. Tsur, Solid State Ionics 188 (2011) 104–109.

Please cite this article as: B.A. Boukamp, A. Rolle, Analysis and Application of Distribution of Relaxation Times in Solid State Ionics, Solid State Ionics (2016), http://dx.doi.org/10.1016/j.ssi.2016.10.009